

Clinical response to larotrectinib in adult Philadelphia chromosome–like ALL with cryptic *ETV6-NTRK3* rearrangement

Valentina Nardi,^{1,2} Nora Ku,³ Matthew J. Frigault,^{1,4} Adrian M. Dubuc,^{1,5} Harrison Kwei Tsai,^{1,5} Philip C. Amrein,^{1,4} Gabriela S. Hobbs,^{1,4} Andrew M. Brunner,^{1,4} Rupa Narayan,^{1,4} Meghan E. Burke,^{1,4} Julia Foster,^{1,4} Paola Dal Cin,^{1,5} Marcela V. Maus,^{1,4} Amir T. Fathi,^{1,4} and Hanno Hock^{1,4,6,7}

¹Harvard Medical School, Boston, MA; ²Department of Pathology, Massachusetts General Hospital, Boston, MA; ³Loxo Oncology, South San Francisco, CA; ⁴Cancer Center, Massachusetts General Hospital, Boston, MA; ⁵Department of Pathology, Brigham and Women's Hospital, Boston, MA; ⁶Center for Regenerative Medicine, Massachusetts General Hospital, Boston, MA; and ⁷Harvard Stem Cell Institute, Cambridge, MA

Key Points

- Larotrectinib has clinical activity in adult Ph-like acute lymphoblastic leukemia with *ETV6-NTRK3* rearrangements.
- *ETV6-NTRK3* rearrangements can be cryptic and subclonal in Ph-like ALL at diagnosis and selected for with aggressive therapy.

Philadelphia chromosome (Ph)–like acute lymphoblastic leukemia (ALL) is a subtype of Ph-negative ALL that molecularly resembles Ph-positive ALL. It shares the adverse prognosis of Ph-positive ALL, but lacks the BCR-ABL1 fusion oncogene. Instead, Ph-like ALL is associated with alternative mutations in signaling pathways. We describe a case of Ph-like ALL that harbored 2 genomic alterations, which activated signaling, an NRASGly12Asp mutation, and an *ETV6-NTRK3* rearrangement. Initially, the *NRAS* mutation was detected at high frequency, whereas the gene fusion was only detectable with a targeted next-generation sequencing-based fusion assay, but not by fluorescence in situ hybridization analysis. The disease failed to respond to multiagent chemotherapy but investigational CD19-directed chimeric antigen receptor T-cell therapy resulted in a complete remission. However, the leukemia relapsed after 6 weeks. Intriguingly, the *NRAS* mutation was extinguished during the chimeric antigen receptor T-cell therapy and did not contribute to the relapse, which was instead associated with a rise in *ETV6-NTRK3*. The relapsed leukemia progressed with further chemo- and immunotherapy but was controlled for 6 weeks with substantial leukemic cytoreduction using the TRK inhibitor larotrectinib. Unfortunately, recovery of normal hematopoiesis was only marginal and the patient eventually succumbed to infections. These results demonstrate that larotrectinib has clinical activity in *ETV6-NTRK3*-associated Ph-like ALL.

Introduction

Treatment and prognosis of Philadelphia chromosome (Ph)⁺–like acute lymphoblastic leukemia (ALL) have markedly improved with drugs targeting the oncogenic tyrosine kinase BCR-ABL1.¹ In Ph[−] ALL, targets for similar small molecule drugs are elusive in most cases. However, 2 research groups identified a subgroup of Ph[−] ALL cases, termed Ph-like ALL or *BCR-ABL1*-like ALL, which resembles Ph⁺ ALL with similar associated mutations including *IKZF1*, similarities in gene expression, and a poor prognosis.^{2,3} Ph-like ALL commonly harbors genomic alterations activating alternative pathways, including ABL, JAK-STAT, RAS, and tropomyosin receptor tyrosine kinase (TRK) signaling.⁴ Some of these have been targeted experimentally and clinically, but the development of optimal treatment strategies is only beginning.⁵ TRK alterations occur in ~1% of cases of Ph-like ALL.⁶

Submitted 29 July 2019; accepted 26 November 2019; published online 6 January 2020. DOI 10.1182/bloodadvances.2019000769.

Send data sharing requests via e-mail to the corresponding author at hock.hanno@mg.harvard.edu.

The full-text version of this article contains a data supplement.

© 2020 by The American Society of Hematology

Methods

Next-generation sequencing of candidate genes associated with hematological malignancies

A clinically validated Anchored Multiplex polymerase chain reaction (PCR)-based assay^{7,8} (Heme SNaPshot v3) was used for the detection of single nucleotide variants and insertion/deletions (indels) in 103 genes recurrently mutated in hematological malignancies, using the ArcherDx platform and Illumina NextSeq next-generation sequencing. Briefly, genomic DNA extracted from bone marrow (BM) aspirate, blood, unstained smears, or FFPE specimens was enzymatically sheared, end-repaired, adenylated, and ligated with a half-functional adapter. A sequencing library targeting hotspots and full exons was generated using 2 heminested PCR reactions. Illumina NextSeq 2 × 151 base paired-end sequencing results were aligned to the hg19 human genome reference. An ensemble-based variant calling approach and a laboratory-developed hotspot caller were applied for single nucleotide variant and indel variant detection.

Fusion detection

A clinically validated Anchored Multiplex PCR-based targeted assay (heme fusion assay v2) was used for detection of fusion transcripts involving genes more commonly rearranged in hematological malignancies using next-generation sequencing.^{8,9} Briefly, total nucleic acid was isolated from blood, BM aspirate, or smears or FFPE tissue. Double-stranded complementary DNA was created then end-repaired, adenylated, and ligated with a half-functional adapter. Two heminested PCR reactions using ArcherDx Heme Fusion kit primers were performed to create a fully functional sequencing library that targets 86 genes (exons). Illumina NextSeq 2 × 151 base paired-end sequencing results were aligned to the hg19 human genome reference with BWA-MEM¹⁰; a laboratory-developed algorithm was then used for fusion transcript detection and annotation through split-read analysis of primary and secondary alignments. Two recurrent *ETV6-NTRK3* isoforms were observed in the fusion data, where the dominant isoform always demonstrated fusion of *ETV6* exon 4 to *NTRK3* exon 15 of the standard transcript of *NTRK3* (NM_001012338.2), whereas the minor isoform demonstrated fusion of *ETV6* exon 4 to *NTRK3* exon 15 of an alternative transcript of *NTRK3* (NM_001007156.2). The ratio of fusion transcripts (spanning the *ETV6-NTRK3* junction of either isoform) over wild-type transcripts (spanning the *ETV6* exon 4 to exon 5 junction) was calculated for each of the time points fusion assay testing was performed.

Cytogenetic analysis and FISH

GTG-banded metaphases were obtained from unstimulated 24-hour BM cultures according to standard cytogenetic protocols. Interphase fluorescence in situ hybridization (FISH) was performed on remaining fixed pellet BM cultures, and on 5-micron FFPE tissue sections from the lymph node specimen slides according to standard genetic protocols and the manufacturer's recommended hybridization conditions. FISH probes were purchased from Abbott Molecular (Des Plaines, IL), Vysis LSI *ETV6* (Cen) and Vysis LSI *ETV6* (Tel) probes at 12p13, to identify any 12p13 rearrangement; Vysis LSI *TP53* SpectrumOrange/CEP17 SpectrumGreen probe at 17p13.1 and D17Z1 at 17p11.1-q11.1 were used to identify del(17p); and centromeric

probes for chromosomes 8 and 9 were used to identify trisomy 8 and monosomy 9, respectively. For *NTRK3* rearrangements we used a break-apart probe set targeting the 5' upstream region (RP11-110O23, green probe) and the 3' downstream region of *NTRK3* (RP11-267B23, red probe). Well-delineated fluorescence signals were screened in at least 100 nuclei and 50 nuclei, on fixed pellets and on 5-micron tissue sections, respectively. In all samples, a considered positive result was based on the cutoff value used by our laboratory for each probe.

Immunohistochemistry

Immunohistochemistry with a pan-TRK (anti-TrkA, anti-TrkB, and anti-TrkC) antibody was performed by Paradigm Diagnostics as described.¹¹

Treatments

Informed consent was obtained for treatment including participation in 3 institutional review board-approved trials (NCT02228772, 17033, 18410).

Results and discussion

A 61-year-old man presented with *Legionella* pneumonia and pancytopenia. Workup established a diagnosis of B-ALL with 95% blasts (Figure 1A-B) positive for CD19, CD10, TdT, CD34, and HLA-DR, but negative for CD20 and myeloperoxidase. Analysis demonstrated an abnormal karyotype, including deletion 17p (*TP53* deletion confirmed by FISH), monosomy 9, and trisomy 10 (Figure 2A), but no t(9;22) or *BCR-ABL1* by reverse transcriptase-PCR. Sequencing⁷ revealed mutations in *IKFZ1* (p.Ser258Ter, variant allelic frequency [VAF] 71.6%), *ETV6* (p.Lys384TyrfsTer11, VAF 52.9%), *CREBBP* (c.3836+2_3836+3insGGGG splice region variant, VAF 45.5%), and *NRAS* (p.Gly12Asp, VAF 40.4%) (Figure 3A). The *IKFZ1* and *ETV6* mutations result in truncated, functionally crippled proteins that act as dominant negatives of the respective normal proteins in B-ALL.^{3,12} *CREBBP* mutations have also been described in B-ALL.¹³ Finally, a targeted RNA-based assay to detect gene fusions (heme fusion assay)⁹ revealed a low amount (29 unique fusion reads) of *ETV6-NTRK3* chimeric transcripts, in which the oligomerization domain of the transcription factor *ETV6* (exons 1-4) is joined to a truncated neutrotrophin-3 receptor (*NTRK3*, exon 15 gene end, including its tyrosine kinase domain), identical to a previously described alteration in a patient with AML¹⁴ (Figure 3B-C; supplemental Figure 1). Unlike the *ETV6* p.Lys384TyrfsTer11 mutation, *ETV6-NTRK3* fusions do not involve the *ETV6* DNA binding domain, so these 2 *ETV6* alterations are independent. Cytogenetic analysis did not reveal the translocation t(12;15)(p13;q25) associated with *ETV6-NTRK3*¹⁵ and, at this early time, we were unable to demonstrate *ETV6* rearrangements by FISH (100 nuclei scored; Figure 3E), indicating that the frequency of the fusion was below the detection limit of these assays. Together, our findings established the diagnosis of Ph-like B-ALL. The low frequency of *ETV6-NTRK3* fusions at diagnosis and early in the course of treatment (Figure 3C-D) suggested that it was initially not the dominant oncogene.

The patient was first treated on a phase 1 study¹⁶ combining the protease inhibitor ixazomib with prednisone, vincristine, doxorubicin, cyclophosphamide, asparaginase, and intrathecal therapy (Figure 1A). This resulted in clearance of blood blasts and recovery of blood counts,

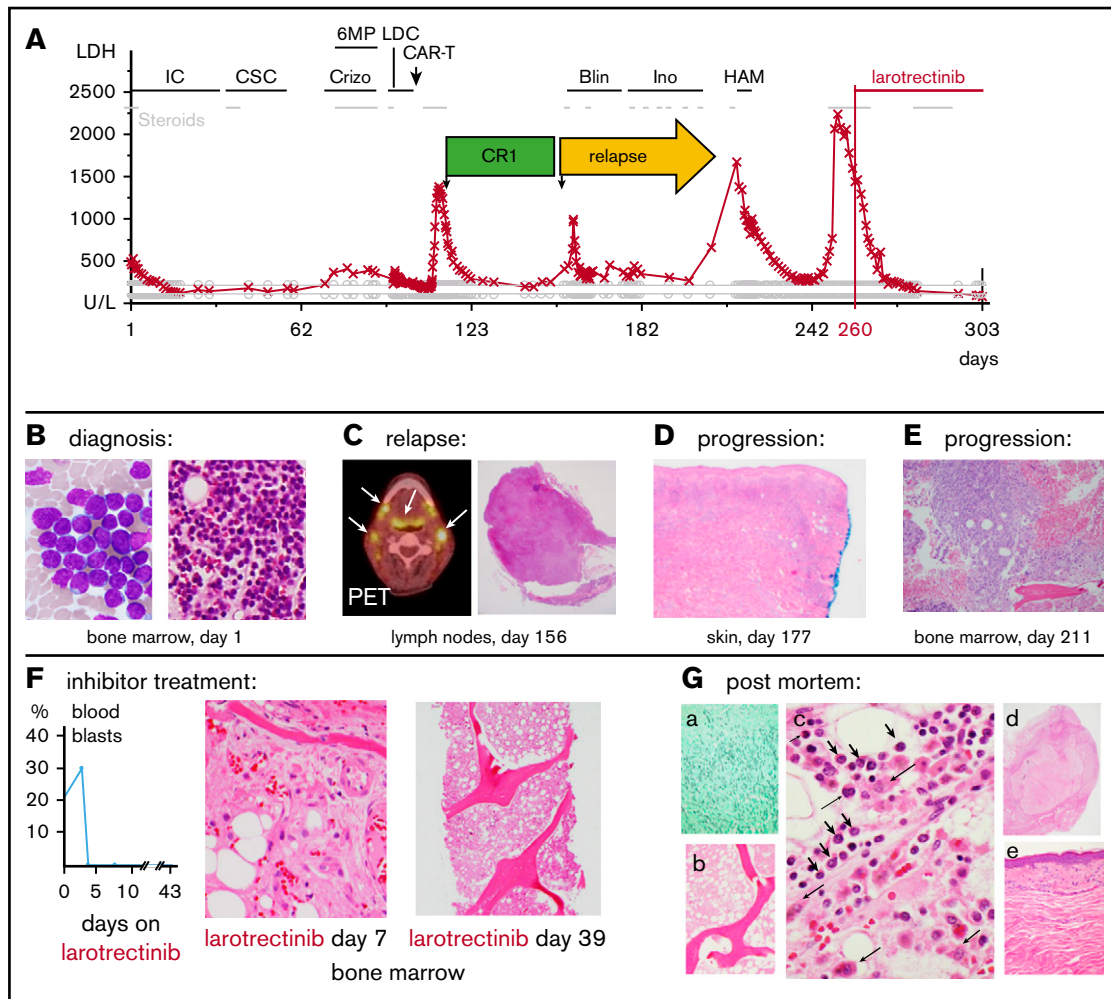


Figure 1. Clinical course and treatment response. (A) Blood LDH levels in synopsis with treatments over time. (B) Initial bone marrow aspirate (left; Wright-Giemsa stain, magnification $\times 100$) and histology (right; hematoxylin and eosin [H&E] stain, magnification $\times 20$). (C) Positron emission tomography scan of the neck with enhanced signal in lymph nodes and lymphoid tissues (left, arrows) and lymph node histology showing leukemia infiltration (right; H&E, magnification $\times 4$). (D) Leukemia cutis in skin biopsy. Magnification $\times 4$. (E) Core biopsy demonstrating bone marrow leukemia in progressive relapse (H&E, magnification $\times 10$). (F) Response to larotrectinib represented by blood blast counts over time (left) and bone marrow biopsy histology (middle and right; H&E, magnification $\times 4$). (G) Autopsy results. (a) Gomori methenamine-silver stain demonstrating invasive aspergillosis. Magnification $\times 20$. (b-c) Bone marrow histology (H&E) showing paucicellular areas, abundant necrosis, rare patches of viable leukemia (short arrows), and histiocytes and myeloid elements (long arrows). Magnification $\times 4$ (b) and $\times 100$ (c). (d) Necrotic lymph node (H&E, magnification $\times 4$). (e) Normal skin (H&E, magnification $\times 10$). (A-G) Days refer to time from diagnosis, except in panel F, which shows days from larotrectinib treatment start. Blin, blinatumomab; Crizo, crizotinib; CSC, consolidation chemotherapy; HAM, high-dose cytarabine and mitoxantrone; IC, induction chemotherapy; Ino, inotuzumab; LDC, lymphodepletion chemotherapy.

but bone marrow biopsies after the first and second therapy cycle revealed refractory disease ($> 70\%$ blasts), so the study treatment was discontinued.

ETV6 FISH in the BM following multiagent chemotherapy revealed 4% rearrangements (day 59 after diagnosis; Figure 3E) suggesting that the clone carrying *ETV6-NTRK3* had increased during therapy. He was then treated with crizotinib (250 mg by mouth twice daily), a multiple kinase inhibitor with activity in experimental *ETV6-NTRK3* models⁴ together with 6MP and steroids (Figure 1A) for 20 days but BM and blood lymphoblast counts increased on therapy. Moreover, *ETV6* FISH revealed 16% rearrangements in the bone marrow (day 80 after diagnosis; Figure 3E), indicating crizotinib failure.

At this point, the patient elected to participate in a trial of an investigational CD19-directed chimeric antigen receptor T-cell

(CAR-T) therapy, which included conditioning chemo-immunotherapy for lymphodepletion (Figure 1A). His CAR-T treatment was complicated by grade 3 cytokine release syndrome and grade 3 neurotoxicity (Lee criteria¹⁷) requiring tocilizumab, anakinra, and steroids, but he rapidly recovered blood production without detectable leukemia. He was discharged home 20 days after infusion in a complete remission (Figure 1A).

At 6 weeks following CAR-T infusion, the patient relapsed with generalized lymphadenopathy confirmed with a biopsy of a cervical lymph node (Figure 1A,C). A BM biopsy demonstrated only minor leukemic involvement ($\sim 7\%$ blasts) with normal blood counts. However, his disease continued to progress despite salvage treatment with blinatumomab¹⁸ (Figure 1A,D; progression with leukemia cutis after less than 3 weeks), inotuzumab¹⁹ (Figure 1A,E;

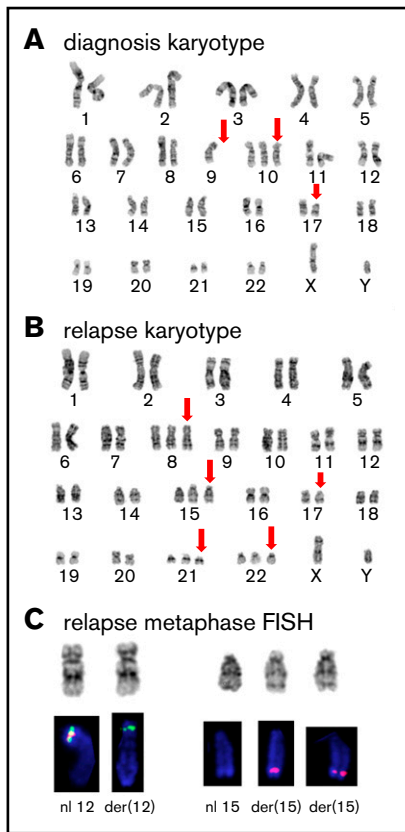


Figure 2. Cytogenetic analysis. (A) GTG-banded representative karyotype at diagnosis showing a 46,XY,-9,+10,del(17)(p11.2) karyotype; abnormal or absent chromosome marked by red arrows. (B) Representative karyotype during relapse showing a 50,XY,+8,+15,del(17)(p11.2),+21,+22 karyotype; abnormal chromosomes marked by red arrows. (C) Partial FISH analysis on chromosomes 12 and 15 demonstrate the cryptic rearrangement t(12;15)(p13q26) and the additional der(15)t(12;15): the 3' *ETV6*(Cen) signal (green) remains on der(12)t(12;15), and 2 copies of the 5' *ETV6*(Tel) signal (red) translocated on 2 copies of der(15)t(12;15).

progression after 4 weeks with pancytopenia and 80% blasts in the bone marrow), and high-dose cytarabine with mitoxantrone²⁰ (Figure 1A; initial myeloablation but persistent pancytopenia followed by rising blood blasts, leukemia cutis, and lymphadenopathy).

Notably, at remission following CAR-T therapy, cytogenetic analysis demonstrated a normal karyotype and mutations were markedly decreased or absent (Figure 3A). At relapse, the *IKFZ1* (VAF, 59.8%), *ETV6* (VAF, 48%), and *CREBBP*-mutations (VAF, 34%) reemerged (Figure 3A). In contrast, the *NRAS* mutation, which persisted after multiagent chemotherapy and was detected at all time points before CAR-T cell therapy, remained undetectable after relapse (VAF, 0%) (Figure 3A). This suggested that it extinguished with the pressure of immunotherapy, consistent with previous data demonstrating that *NRAS* mutations can be selected against or persist during chemotherapy in different circumstances.²¹

Cytogenetic analysis after relapse revealed a second cytogenetically related subclone that was not detected early in the disease. Specifically, the analysis demonstrated persistence of 17p loss, but acquisition of additional chromosomes 8, 14, 21,

and 22 and absence of the chromosome 9 deletion detected at diagnosis (Figure 2B). Subsequently, metaphase FISH studies confirmed that this second clone exhibited a cryptic t(12;15) consistent with the *ETV6-NTRK3* rearrangement (Figure 2C). Moreover, analysis of data from the fusion assay revealed that fusion transcripts (*ETV6* exon 4–*NTRK3* exon 15) increased sharply compared with unrearranged *ETV6* transcript (*ETV6* exon 4–*ETV6* exon 5) after relapse (Figure 3D). Consistent with this, *ETV6* rearrangements were detectable by interphase FISH in 45/50 blast nuclei off/from the lymph node (Figure 2E–F) and, similarly, *NTRK3* rearrangements were demonstrated in 50/50 blast nuclei from the lymph node (Figure 3G). Accordingly, immunohistochemistry confirmed TRK protein expression, which is absent in normal lymphoid tissue¹¹ (Figure 2H). Together, these data suggest that the relapse was associated with an expansion of an *ETV6-NTRK3* rearranged subclone.

Based on these findings, the patient enrolled on a single-patient protocol in an expanded access program for larotrectinib, an agent with activity against *ETV6-NTRK3*-driven solid tumors²² (Figure 1A,F). At the start of oral monotherapy treatment (100 mg twice per day), he had a poor performance status (Eastern Cooperative Oncology Group performance scale 4). By day 4 of treatment, peripheral blood blasts became undetectable (Figure 1F). On day 6, palpable lymphadenopathy and leukemia cutis resolved and a biopsy revealed an ablated BM with only a few scattered blasts (Figure 1F). By day 15, the lactic dehydrogenase (LDH) blood levels, which had correlated with disease activity,²³ had normalized (Figure 1A). He did experience clinical benefit, had no apparent side effects, and was able to spend a week at home. The leukemia did not overtly return during 42 days of larotrectinib treatment, and the patient's LDH level remained normal (Figure 1A). However, blood counts showed only little recovery, and the patient eventually succumbed to multifocal angioinvasive aspergillosis (Figure 1Ga). The autopsy showed extensive tumor necrosis in the BM with rare areas of viable leukemic cells and very rare areas with nonleukemic hematopoietic activity (Figure 1Gb-c). The lymph nodes showed extensive necrosis without viable leukemia, and no leukemia cutis was seen. (Figure 1Gd-e). Sequencing of the *NTRK3* kinase domain did not show larotrectinib resistance-associated mutations, specifically p.G623R and p.G696A.²⁴

In conclusion, we demonstrate that larotrectinib has powerful clinical activity in a case of Ph-like ALL with an *ETV6-NTRK3* fusion in agreement with preclinical studies.^{6,25-27} The case emphasizes the necessity for aggressively searching for pathogenic fusions that can be cytogenetically cryptic. Moreover, it highlights the importance of treatment timing. *ETV6-NTRK3* was initially not the dominant mutation and barely detectable. Yet, it was selected with multiple chemo- and immunotherapies and, ultimately, drove the relapse. We speculate that earlier treatment with larotrectinib might result in better outcomes. The failure of blood cell recovery was likely related to his multiple lines of prior treatment because myelosuppression was not frequently seen with larotrectinib during the treatment of solid tumors.²² Because larotrectinib has very recently been approved for *NTRK* fusion-associated solid tumors irrespective of histology,²⁸ it is now more accessible, and our data reinforce that its use in Ph-like ALL should be further explored.

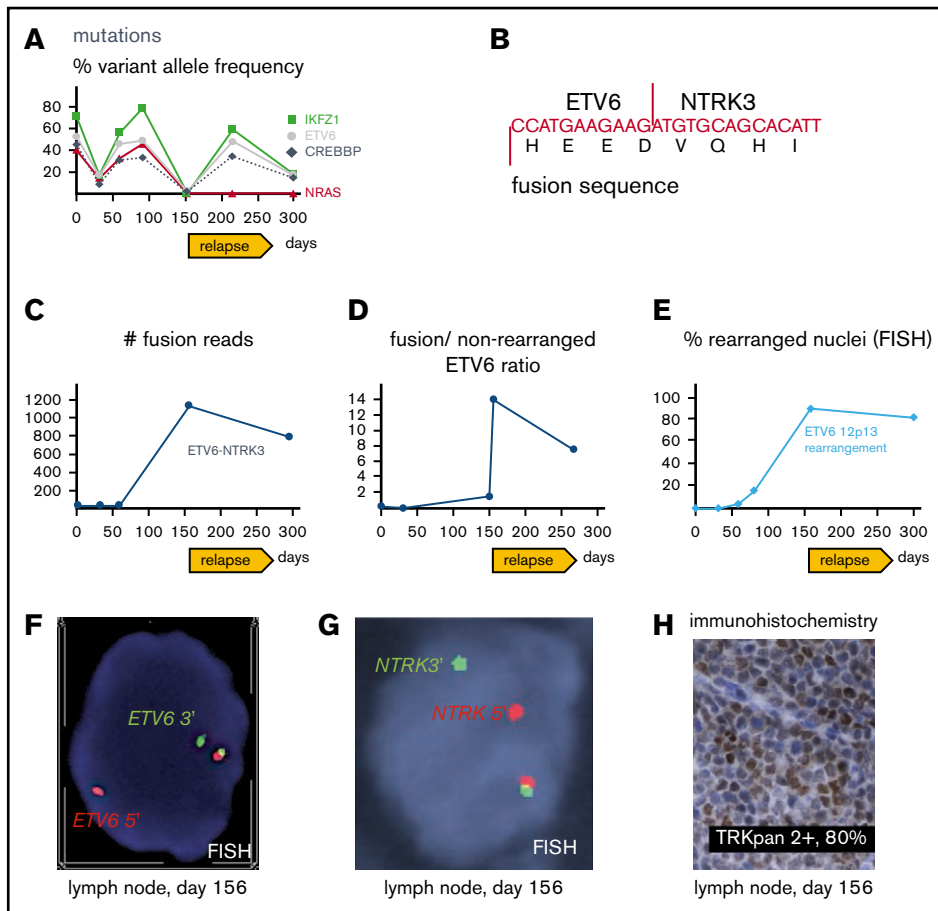


Figure 3. Molecular pathology results. (A) Targeted next-generation sequencing of DNA from bone marrow aspirates with allelic frequency of pathogenic mutations. (B) Sequence of *ETV6-NTRK3* transcript revealed with the fusion assay; for more detailed information, see supplemental Figure 1. (C) Number of unique *ETV6-NTRK3* fusion reads in bone marrow aspirates (days 1, 32, 59, 295) and lymph node (day 156). (D) Ratio of fusion transcripts (*ETV6* exon 4-*NTRK3* exon 15) over wild-type transcript (*ETV6* exon 4-*ETV6* exon 5) from bone marrow aspirates (days 1, 32, 150, 266) and lymph node (day 156). (E) FISH of bone marrow aspirates (day 1, 32, 59, 80, 295) and lymph node (day 156). (F) FISH from lymph node showing break apart of 5' (red) and 3' (green) *ETV6* probes revealing rearrangement as split-apart red and green signals as well the normal locus (unseparated red-green pair with yellow overlap). Magnification $\times 100$. (G) FISH from lymph node showing break apart of 5' (red) and 3' (green) probes recognizing regions upstream and downstream of *NTRK3*, respectively; rearrangement resulting in split-apart red and green signals as well the normal locus (unseparated pair with yellow overlap). Magnification $\times 100$. (H) Immunohistochemical stain revealing aberrant expression of TRK in lymph node. Magnification $\times 40$. (A-H) Days refer to time from diagnosis.

Acknowledgments

The authors thank the patient and his family for participation in research studies. The authors also thank Cynthia McLaughlin and Casey Keagan for expert technical assistance and Aura Ramos and Tina Som for clinical research support.

H.H. was supported by a Hyundai Hope on Wheels Scholar Grant.

Authorship

Contribution: V.N. and H.H. made figures, designed research, and wrote the paper; N.K., M.E.B., and H.H. wrote the larotrectinib

protocol; V.N., A.M.D., H.K.T., and P.D.C. performed experiments; and all authors interpreted data and edited the manuscript.

Conflict-of-interest disclosure: N.K. is employed by Loxo Oncology, a subsidiary of Eli Lilly. The remaining authors declare no competing financial interests.

ORCID profiles: G.S.H., 0000-0002-0199-9333; M.V.M., 0000-0002-7578-0393.

Correspondence: Hanno Hock, Massachusetts General Hospital Cancer Center, 185 Cambridge St, CPZN 4212, Boston, MA 02114; e-mail: hock.hanno@mgh.harvard.edu.

References

- Richard-Carpentier G, Kantarjian H, Jabbour E. Recent advances in adult acute lymphoblastic leukemia. *Curr Hematol Malig Rep*. 2019;14(2):106-118.
- Den Boer ML, van Slegtenhorst M, De Menezes RX, et al. A subtype of childhood acute lymphoblastic leukaemia with poor treatment outcome: a genome-wide classification study. *Lancet Oncol*. 2009;10(2):125-134.

3. Mullighan CG, Su X, Zhang J, et al; Children's Oncology Group. Deletion of IKZF1 and prognosis in acute lymphoblastic leukemia. *N Engl J Med.* 2009; 360(5):470-480.
4. Roberts KG, Li Y, Payne-Turner D, et al. Targetable kinase-activating lesions in Ph-like acute lymphoblastic leukemia. *N Engl J Med.* 2014;371(11): 1005-1015.
5. Roberts KG. Why and how to treat Ph-like ALL? *Best Pract Res Clin Haematol.* 2018;31(4):351-356.
6. Roberts KG, Janke LJ, Zhao Y, et al. ETV6-NTRK3 induces aggressive acute lymphoblastic leukemia highly sensitive to selective TRK inhibition. *Blood.* 2018;132(8):861-865.
7. Boiocchi L, Hasserjian RP, Pozdnyakova O, et al. Clinicopathological and molecular features of SF3B1-mutated myeloproliferative neoplasms. *Hum Pathol.* 2019;86:1-11.
8. Zheng Z, Liebers M, Zhelyazkova B, et al. Anchored multiplex PCR for targeted next-generation sequencing. *Nat Med.* 2014;20(12):1479-1484.
9. Jeck WR, Lee J, Robinson H, Le LP, Iafrate AJ, Nardi V. A nanopore sequencing-based assay for rapid detection of gene fusions. *J Mol Diagn.* 2019; 21(1):58-69.
10. Li H. Aligning sequence reads, clone sequences and assembly contigs with BWA-MEM. *arXiv.* 2013;1303.3997.
11. Rudzinski ER, Lockwood CM, Stohr BA, et al. Pan-Trk immunohistochemistry identifies NTRK rearrangements in pediatric mesenchymal tumors. *Am J Surg Pathol.* 2018;42(7):927-935.
12. Hock H, Shimamura A. ETV6 in hematopoiesis and leukemia predisposition. *Semin Hematol.* 2017;54(2):98-104.
13. Mullighan CG, Zhang J, Kasper LH, et al. CREBBP mutations in relapsed acute lymphoblastic leukaemia. *Nature.* 2011;471(7337):235-239.
14. Eguchi M, Eguchi-Ishimae M, Tojo A, et al. Fusion of ETV6 to neurotrophin-3 receptor TRKC in acute myeloid leukemia with t(12;15)(p13;q25). *Blood.* 1999;93(4):1355-1363.
15. Knezevich SR, Garnett MJ, Pysher TJ, Beckwith JB, Grundy PE, Sorensen PH. ETV6-NTRK3 gene fusions and trisomy 11 establish a histogenetic link between mesoblastic nephroma and congenital fibrosarcoma. *Cancer Res.* 1998;58(22):5046-5048.
16. Amrein PC, Ballen KB, Blonquist TM, et al. Phase I study of ixazomib in addition to chemotherapy for the treatment of acute lymphoblastic leukemia in older adults [abstract]. *Blood.* 2018;132(suppl 1). Abstract 2704.
17. Lee DW, Gardner R, Porter DL, et al. Current concepts in the diagnosis and management of cytokine release syndrome [published correction appears in *Blood.* 2015;126(8):1048]. *Blood.* 2014;124(2):188-195.
18. Kantarjian H, Stein A, Gökbüget N, et al. Blinatumomab versus chemotherapy for advanced acute lymphoblastic leukemia. *N Engl J Med.* 2017;376(9): 836-847.
19. Kantarjian HM, DeAngelo DJ, Stelljes M, et al. Inotuzumab ozogamicin versus standard therapy for acute lymphoblastic leukemia. *N Engl J Med.* 2016; 375(8):740-753.
20. Hiddemann W, Kreutzmann H, Donhuijsen-Ant R, Planker M, Wendt FC, Büchner T. High-dose cytosine arabinoside and mitoxantrone (HAM) for the treatment of refractory acute lymphoblastic leukemia. *Onkologie.* 1987;10(1):11-12.
21. Oshima K, Khiabanian H, da Silva-Almeida AC, et al. Mutational landscape, clonal evolution patterns, and role of RAS mutations in relapsed acute lymphoblastic leukemia. *Proc Natl Acad Sci USA.* 2016;113(40):11306-11311.
22. Drilon A, Laetsch TW, Kummar S, et al. Efficacy of larotrectinib in TRK fusion-positive cancers in adults and children. *N Engl J Med.* 2018;378(8): 731-739.
23. Kornberg A, Polliack A. Serum lactic dehydrogenase (LDH) levels in acute leukemia: marked elevations in lymphoblastic leukemia. *Blood.* 1980;56(3): 351-355.
24. Cocco E, Scaltriti M, Drilon A. NTRK fusion-positive cancers and TRK inhibitor therapy. *Nat Rev Clin Oncol.* 2018;15(12):731-747.
25. Li Z, Tognon CE, Godinho FJ, et al. ETV6-NTRK3 fusion oncogene initiates breast cancer from committed mammary progenitors via activation of AP1 complex. *Cancer Cell.* 2007;12(6):542-558.
26. Taylor J, Pavlick D, Yoshimi A, et al. Oncogenic TRK fusions are amenable to inhibition in hematologic malignancies. *J Clin Invest.* 2018;128(9): 3819-3825.
27. Vaishnavi A, Capelletti M, Le AT, et al. Oncogenic and drug-sensitive NTRK1 rearrangements in lung cancer. *Nat Med.* 2013;19(11):1469-1472.
28. Huang FW, Feng FY. A tumor-agnostic NTRK (TRK) inhibitor. *Cell.* 2019;177(1):8.